THE JOURNAL OF BIOLOGICAL CHEMISTRY
Vol. 269, No. 41, Issue of October 14, pp. 25315–25320, 1994
Printed in U.S.A.

Modeling the Bacterial Protein Toxin, Pneumolysin, in Its Monomeric and Oligomeric Form*

(Received for publication, July 18, 1994)

Peter J. Morgan‡§, Stefan C. Hyman¶, Olwyn Byron‖, Peter W. Andrew‡, Timothy J. Mitchell‡, and Arthur J. Rowe‖

From the ‡Department of Microbiology and Immunology, University of Leicester, Leicester LE1 9HN, ‖NCMH, Department of Biochemistry, University of Leicester, Leicester LE1 7RH, and the ¶Electron Microscope Laboratories, School of Biological Sciences, Leicester University, Leicester LE1 7RH, United Kingdom

Pneumolysin is a member of the family of related bacterial thiol-activated toxins, which share structural similarities and a proposed common cytolytic mechanism. Currently the molecular mechanism of membrane damage caused by these toxins remains a matter of controversy. A prerequisite for defining this mechanism is a detailed knowledge of the monomeric and oligomeric pneumolysin structures.

We present for the first time details of the monomeric structure of a thiol-activated toxin, pneumolysin. Electron microscope images of metal-shadowed pneumolysin monomers show an asymmetric molecule composed of four domains. We have studied the conformation of pneumolysin monomer by low resolution hydrodynamic bead modeling procedures. The bead model dimensions and shape are derived solely from the electron micrographs. The bead model has been evaluated in terms of the predicted solution properties, which in turn have been compared to the experimental values of the sedimentation coefficient, $s^0_{20,w}$, obtained by analytical ultracentrifugation and the intrinsic viscosity, [η]. Pneumolysin oligomers, observed as ring- and arc-shaped structures, were also examined by electron microscopy. Metal shadowing and negative staining methods were used to establish the overall dimensions of the oligomer and were used to produce a morphological model for the oligomer, incorporating monomer subunits based on the hydrodynamic bead model.

The membrane-damaging toxin pneumolysin is an important virulence factor of the bacterium *Streptococcus pneumoniae* (Berry *et al.*, 1989). This bacterium is a major pathogen of man and commonly causes pneumonia, meningitis, and otitis media (Austrian, 1981). Pneumolysin is one of the so-called thiol-activated toxins, which are produced by a broad range of Gram-positive bacteria and which share a large number of structural characteristics and biological properties (Alouf and Geoffroy, 1991).

One of the most noted effects of pneumolysin is the cytolysis of eucaryotic cells, which contain cholesterol in their membranes. It has been suggested that cholesterol acts as the membrane receptor for these toxins and facilitates the concentration and resulting oligomerization of toxin monomers in the membrane (Bhakdi *et al.*, 1985). This results in the formation of the classical ring and arc structures that have been reported for many of the thiol-activated toxins (Dourmashkin and Rosse, 1966; Duncan and Schlegel, 1975; Cowell *et al.*, 1978; Mitsui *et al.*, 1979; Rottem *et al.*, 1982; Niedermeyer, 1985). We have recently presented (Morgan *et al.*, 1994) a preliminary study, which shows, for the first time, the formation of these ring and arc structures by pneumolysin. A number of previous papers have proposed models for the oligomeric structure of these rings and arcs (Bhakdi *et al.*, 1985; Niedermeyer *et al.*, 1985; Duncan and Schlegel, 1975; Sekiya *et al.*, 1993), but all have lacked essential information concerning the size and conformation of the building block, the toxin monomer.

We present a detailed analysis of the oligomeric structures, obtained by use of electron microscopy techniques. The same techniques have been applied to the pneumolysin monomer, and based on these studies we are able to propose a hydrodynamic bead model for the monomer structure. The intrinsic viscosity of pneumolysin has been determined and, in common with the previously determined sedimentation coefficient (Morgan *et al.*, 1993), is in close agreement with the value predicted for the model. This monomeric model provides the essential information necessary for constructing the assembled form of pneumolysin, and on this basis we are able to propose a model for the gross structure of the pneumolysin oligomer.

MATERIALS AND METHODS

Reagents—All chemicals used were analytical grade (Fisons) unless otherwise stated. All protein samples were dissolved in phosphate-buffered saline (8 mM Na_2HPO_4, 1.5 mM KH_2PO_4, 0.137 M NaCl, 2.5 mM KCl, pH 7.3).

Expression and Purification of Recombinant Wild-type Pneumolysin—Recombinant pneumolysin protein was purified from *Escherichia coli* JM101 and purified as described previously (Mitchell *et al.*, 1989). Sample purity was checked by SDS-polyacrylamide gel electrophoresis and hemolytic activity assayed as described previously (Mitchell *et al.*, 1989).

Isolation of Pneumolysin Oligomers—Isolated oligomeric pneumolysin was prepared as described previously in Saunders *et al.*, 1989. One milliliter of sheep red blood cells (10^9 cells) were incubated with 50 μg of purified wild-type pneumolysin for 5 min at 37 °C. Membranes were pelleted by centrifugation (25,000 × *g*, 15 min, 4 °C) and washed three times with 5 mM phosphate buffer (pH 8.0) to lyse any remaining intact cells. Membranes were solubilized by addition of sodium deoxycholate to a concentration of 250 mM. Samples of 1 ml were applied to linear 10–40% (w/v) sucrose density gradients containing 6.25 mM sodium deoxycholate as described previously (Bhakdi *et al.*, 1985). After centrifugation at 150,000 × *g* for 16 h at 4 °C (Sorvall AH-627 with swing-out rotor), 10 fractions (1 ml each) were collected by puncturing the bottom of the tubes. Fractions were analyzed for the presence of pneumolysin by SDS-polyacrylamide gel electrophoresis.

Electron Microscopy—For negative staining, samples of pneumolysin were vapor-fixed for 1 min over glutaraldehyde solution, prior to rinsing with distilled water and contrasting with either 0.8% (w/v) sodium

* This work was supported by the United Kingdom Medical Research Council, The Royal Society, and the Biotechnology and Biological Sciences Research Council. The costs of publication of this article were defrayed in part by the payment of page charges. This article must therefore be hereby marked "*advertisement*" in accordance with 18 U.S.C. Section 1734 solely to indicate this fact.

§ To whom correspondence should be addressed: Dept. of Microbiology and Immunology, University of Leicester, P. O. Box 138, University Rd., Leicester LE1 9HN, United Kingdom. Tel.: 533-523018; Fax: 533-525030.

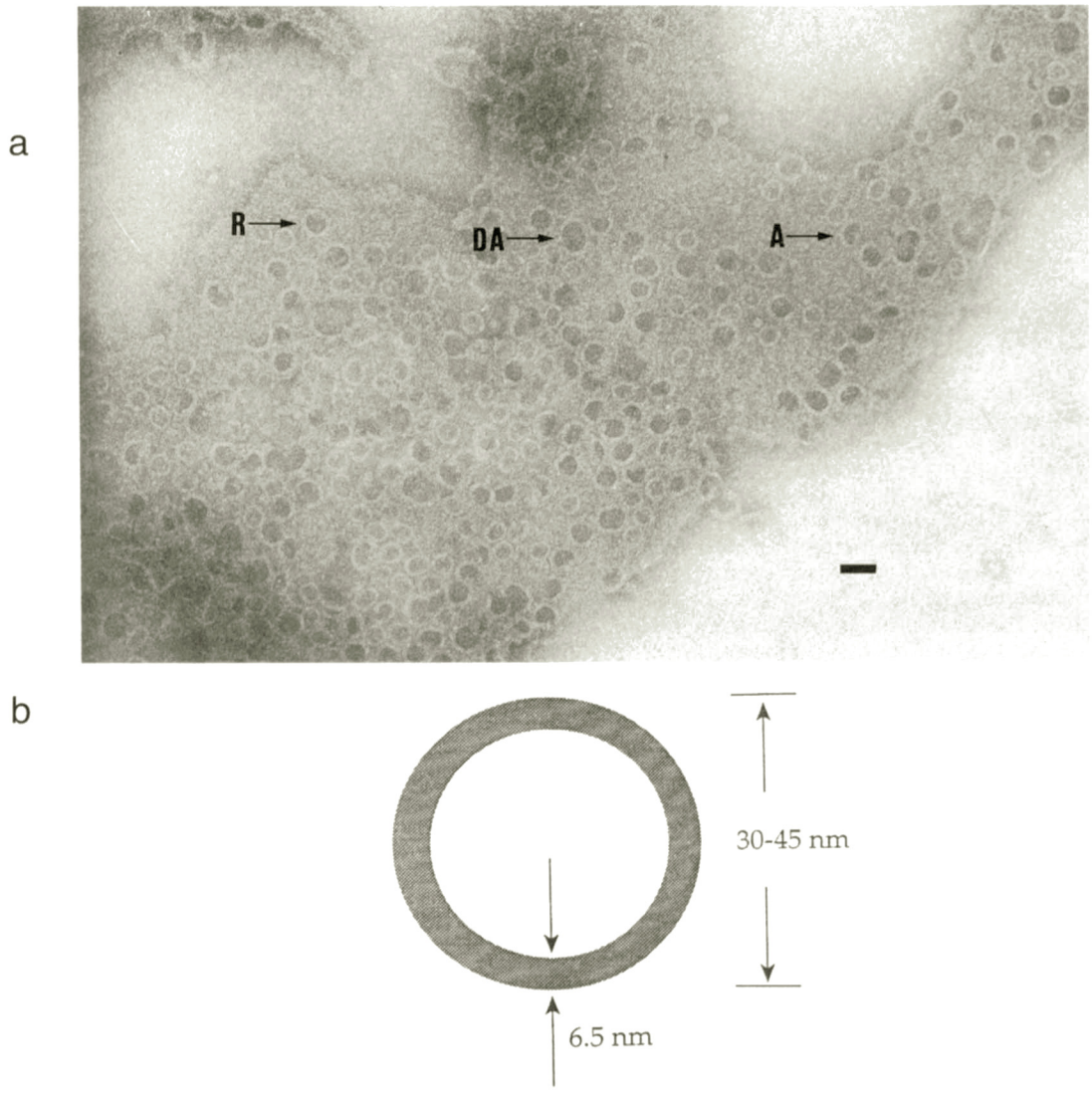

FIG. 1. *Panel a*, sheep erythrocyte membrane treated with pneumolysin. Erythrocytes (2.0%, v/v) were treated with pneumolysin (0.2 mg ml^{-1}) at 37.0 °C for 20 min. Membranes were obtained by centrifugation at 11,000 × *g* for 20 min and negatively stained. Magnification × 133,000; *bar* = 50 nm. *Arrow R*, rings; *arrow A*, arcs; *arrow DA*, double arcs. *Panel b*, schematic of oligomeric ring showing dimensions.

phosphotungstate, pH 6.8, or unbuffered 2% (w/v) uranyl acetate. For metal shadowing, samples of pneumolysin at various concentrations in 50% (w/w) glycerol were sprayed onto freshly cleaved mica, and after drying for 15 min at 10^{-5} millibar were shadowed with platinum at low angle (5°) unidirectionally. Replicas were floated off onto distilled water. All specimens were examined and photographed in a Siemens 102 transmission electron microscope, with the magnification calibrated using a diffraction grating replica. Electron micrographs were measured on an Apple digitizer. At least 30 measurements were made of each dimension.

Intrinsic Viscosity Determination—The kinematic reduced viscosity ($[\eta'_{red}]$) of pneumolysin monomer was determined for a range of protein concentrations using a micro-Ostwald viscometer. The pneumolysin was dissolved in 40% (w/w) glycerol in order to maximize the viscosity increment arising from the macromolecular solute (Szuchet and Johnson, 1966). Flow times were measured automatically on a Schott Geräte AVS 400 apparatus. The sample was maintained at 20.0 ± 0.01 °C by a thermostatically controlled water bath. The dynamic intrinsic viscosity, $[\eta]$, was calculated from the corresponding kinematic value $[\eta']$ by using Tanford's correction formula (Tanford, 1955), where ρ_0 is the density of the solvent and $\bar{v}$ is the partial specific volume of pneumolysin.

$$[\eta] = \frac{(1 - \bar{v}\rho_0)}{\rho_0} + [\eta'] \qquad \text{(Eq. 1)}$$

Bead Modeling—In order to interpret the solution data acquired for pneumolysin monomer (Morgan *et al.*, 1993), a low resolution bead model was constructed and tested with hydrodynamic bead modeling (García de la Torre and Bloomfield, 1981). The arrangement of beads in the model was based on the appearance of monomer in electron micrographs, from which measurements of domain size and interdomain distances were made.

Thus, the anhydrous model consists of four equally sized beads of radius 1.54 nm. The translational frictional coefficient (f_T) and intrinsic viscosity ($[\eta]$) for this model were calculated using the TRV program (García de la Torre, 1989), which was run on the Silicon Graphics Instruments Challenge XL mainframe computer at the University of Leicester.

RESULTS

Interaction with Erythrocyte Membranes—Negatively stained preparations of sheep erythrocytes treated with pneumolysin reveal large numbers of arc and ring structures on their surface (Fig. 1*a*). The number of arcs and rings appeared to be in proportion to the concentration of toxin used. The structures appeared to fall into three main categories: rings, arcs, and "double arcs" (Fig. 1*a*, see *arrows*). The ring width (see Fig. 1*b*) was found to measure 6.5 nm (S.D. ± 0.3 nm) regardless of which category of structure it formed. The outer diameter of the rings vary in size from 30 to 45 nm. The radii of curvature of the arcs appear the same as the ring structures.

Isolated Oligomers—Oligomers were isolated from pneumolysin-treated membranes by sucrose density gradient centrifu-

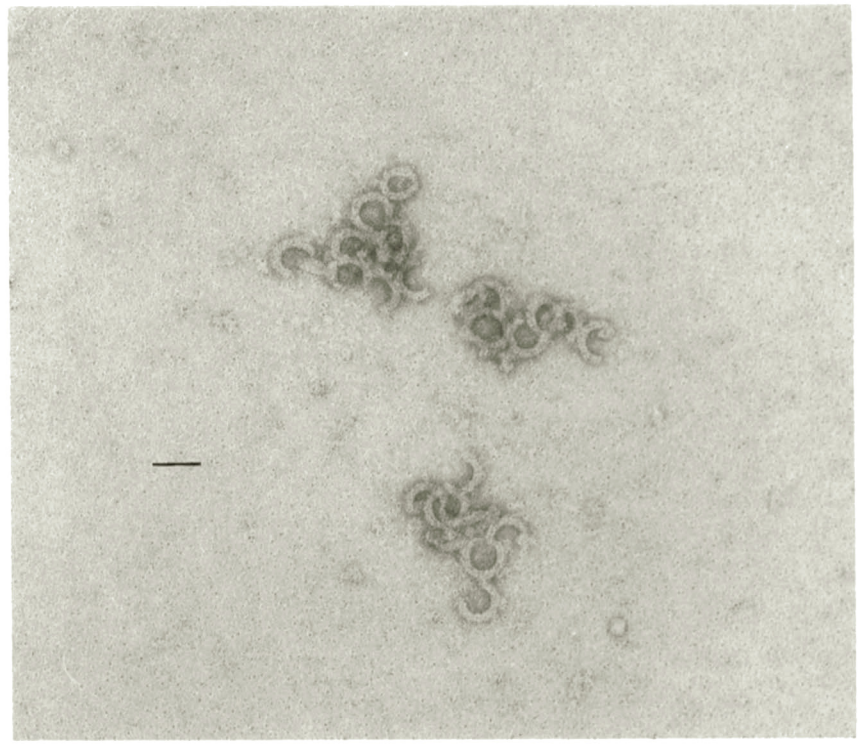

FIG. 2. **Pneumolysin oligomers isolated from sheep erythrocytes and negatively stained.** Magnification × 212,000; *bar* = 40 nm.

gation. The isolated structures were prepared by various electron microscopy techniques. Preparations of the isolated oligomers that were negatively stained with uranyl acetate or sodium phosphotungstate revealed ring and arc structures identical to those seen in membranes (Fig. 2).

The oligomers were linearly shadowed on mica with platinum and carbon and the replica viewed (Fig. 3*a*). As with the negatively stained isolated oligomers, the dimensions were the same as those found in membranes. By measuring the length of the shadows created by the oligomers, an estimate for the height of the oligomers was determined. Tobacco mosaic virus was used for calibration purposes to accurately determine the angle of shadowing and the oligomer height was calculated as 9.3 nm (S.D. ± 1.6 nm). The absence of shadowing metal inside the oligomeric ring confirms the presence of a central hole. At high magnification (Fig. 3*b*), the ring- and arc-shaped structures appear to be composed of subunits, presumably pneumolysin monomer.

Molecular Shape of Pneumolysin—High magnification micrographs of platinum/carbon-coated pneumolysin reveal the apparent domain structure of the monomeric protein (Fig. 4*a*). The pneumolysin molecules are asymmetric as opposed to globular and are slightly curved. The individual protein molecules appear to be composed of four domains, three of which are linearly associated, with the fourth observed at a range of angles. This may imply flexible linkage with respect to the other three. The center-to-center distance between domains was measured as 3.08 nm (S.D. ± 0.65 nm) and the overall projected length of the monomers was 12.56 nm (S.D. ± 0.49 nm).

Viscometry—Extrapolating the kinematic reduced viscosity to infinite dilution yielded a value of 9.1 ± 0.5 ml/g for the dynamic intrinsic viscosity, $[\eta]$, of pneumolysin monomer (see Fig. 5). $[\eta]$ is a particularly sensitive probe of solution conformation but is also highly dependent upon molecular hydration (δ). The shape contribution to $[\eta]$ is represented by the Simha factor (ν) (Tanford, 1963), and the two are related through the following equation, where v^0 is the specific volume of pure solvent.

$$[\eta] = \nu(\bar{v} + \delta v^0) \qquad \text{(Eq. 2)}$$

DISCUSSION

We are able to confirm preliminary data presented previously (Morgan *et al.*, 1994) to show that pneumolysin forms the ring and arc structures traditionally associated with the thiol-activated toxins. Further detailed examination of these structures shows that the dimensions of the pneumolysin oligomers are very similar to those reported for the other toxins that have been investigated (Dourmashkin and Rosse, 1966; Duncan and Schlegel, 1975; Cowell *et al.*, 1978; Mitsui *et al.*, 1979; Rottem *et al.*, 1982; Niedermeyer, 1985). This is to be expected considering their primary structure and function similarities. The oligomeric structures display extraordinary stability and remain intact and, as the micrograph in Fig. 2. reveals, have a tendency to aggregate.

Surprisingly little information is available concerning the detailed structure of the oligomers from this family of toxins. The most comprehensive model for a thiol-activated toxin oligomer was presented recently for streptolysin O (Sekiya *et al.*, 1993). This model was derived from enhanced images of electron micrographs of negatively stained streptolysin O oligomers. These workers proposed that the oligomeric structure is composed of an outer and an inner layer of monomer subunits and that a "crown" portion of the monomer projects out from the cell membrane. However, the presence of two concentric rings of monomer subunits is unique to the streptolysin O model. This proposal does not conform to the basic packing principle of organized structures, which states that "each subunit must be bonded to its neighbour in exactly the same way; thus all subunits are in identical environments" (Klug, 1969). We can see that for the kind of model proposed for streptolysin O, the monomer subunits in the outer ring are not in the same environment as those in the inner ring and *vice versa*.

Enhanced image processing of electron micrographs was also employed (Olofsson *et al.*, 1993) to study perfringolysin oligomers. The final projection density map presented does appear to show two concentric layers of units, although based on volumetric considerations (derived from monomer molecular weight) the authors conclude that the monomer subunit spans

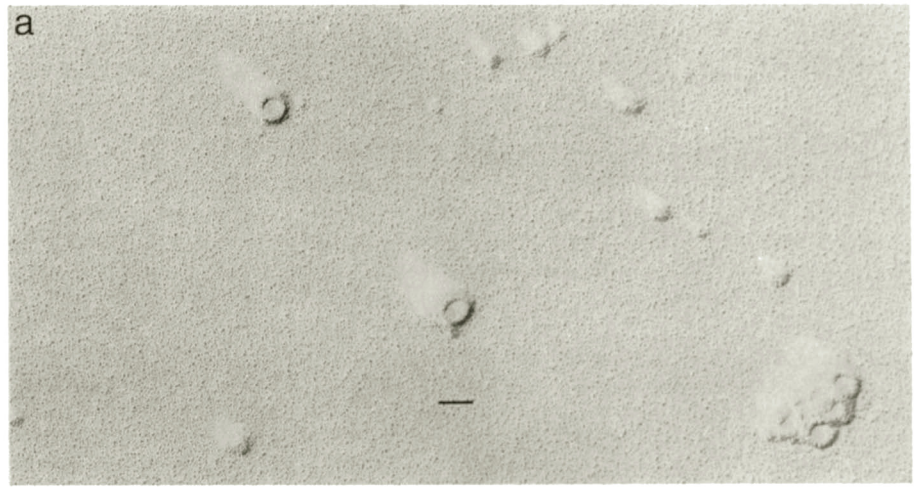

FIG. 3. *Panel a*, pneumolysin oligomers isolated from sheep erythrocytes and metal-shadowed. Magnification × 133,000; *bar* = 50 nm. *Panel b*, as for *panel a* but higher magnification (× 423,000).

the width of the ring. Another study of perfringolysin (Harris *et al.*, 1991), in which the technique of fluorescence resonance energy transfer was used to monitor the kinetic aspects of aggregation, suggests that perfringolysin O aggregates in a linear fashion and would seem to preclude the two-ring model. A number of other models have been proposed (Bhakdi *et al.*, 1985; Niedermeyer *et al.*, 1985; Duncan and Schlegel, 1975). In general, the proposed models have been generated using an assumed thickness for the oligomeric structure. More importantly, to date there has been no structural information concerning the toxin monomer, the primary building block of the oligomeric structure.

For this reason we have constructed a bead model of the pneumolysin monomer (Fig. 4*b*) based on measurements taken from electron micrographs of low angle, finely metal-shadowed pneumolysin (seen in Fig. 4*a*). The molecules appear to be ~5.0 nm in width, although this value is incompatible with the well characterized overall length and volume. It should be noted that measuring dimensions in the direction of the shadow can be very misleading due to metal deposition, which can vary considerably (as much as 1–4 nm), in which case the thickness of the deposited metal can be of a similar order to the structure being measured. However, dimensions perpendicular to the direction of shadow along the length of the molecule may be measured quite accurately by this method. The bead model representation of the pneumolysin monomer presented in Fig. 4*b* is based on these measurements. The size of each domain is based on the center-to-center distance between domains (3.08 nm) along the length of the molecule, and the assumption has been made that they are spherical. In this model, pneumolysin is composed of four domains of equal size where one end domain is flexible with respect to the axis of the other three.

The use of simple equations (Rowe, 1984) allows the calculation of a molecular weight, based on the volume of the individual domains (as estimated from electron micrographs) and the partial specific volume of pneumolysin. The partial specific volume of 0.737 ml/g was derived from the amino acid composition (Morgan *et al.*, 1993). The calculated value of 50,000 agrees well with the sequence molecular weight of 52,900, suggesting that in terms of volume the model is a good representation of the molecule.

Using low resolution bead modeling analysis (García de la Torre, 1989), it is possible to predict theoretical parameters based on the proposed bead representation, molecular weight, and partial specific volume. The dependence of both the sedimentation coefficient and intrinsic viscosity upon model hydration and flexibility was probed for a range of hydrations (0.0–1.4 g of water/g of protein) and intersegment angles (180, 135, and 90°), as illustrated in Fig. 6 (*a* and *b*). We have addressed the issue of flexibility in a manner somewhat different than that of other workers in this area (Rocco *et al.*, 1993), in that we have not attempted to generate a series of models for the mon-

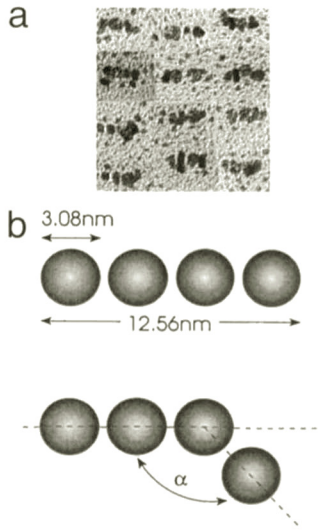

FIG. 4. *Panel a*, composite of electron micrographs of unidirectionally metal-shadowed pneumolysin monomers. Magnification × 855,000. *Panel b*, hydrodynamic bead model of pneumolysin monomer constructed to the dimensions measured from electron micrographs in *panel a*. The bead model has a total volume compatible with the known molecular volume of pneumolysin.

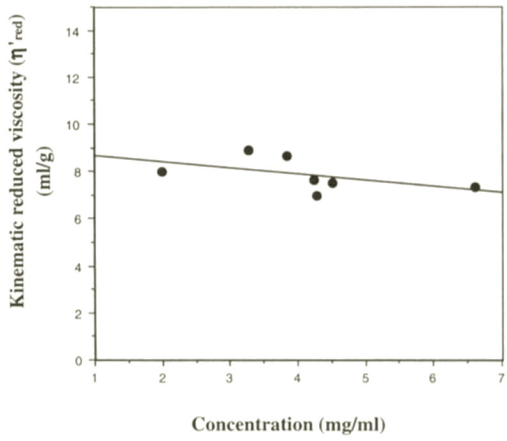

FIG. 5. **Kinematic reduced viscosity, $[\eta'_{red}]$, *versus* concentration for pneumolysin monomer.** The slight negative regression, although barely significant, suggests a very slight degree of self-association with increasing concentration.

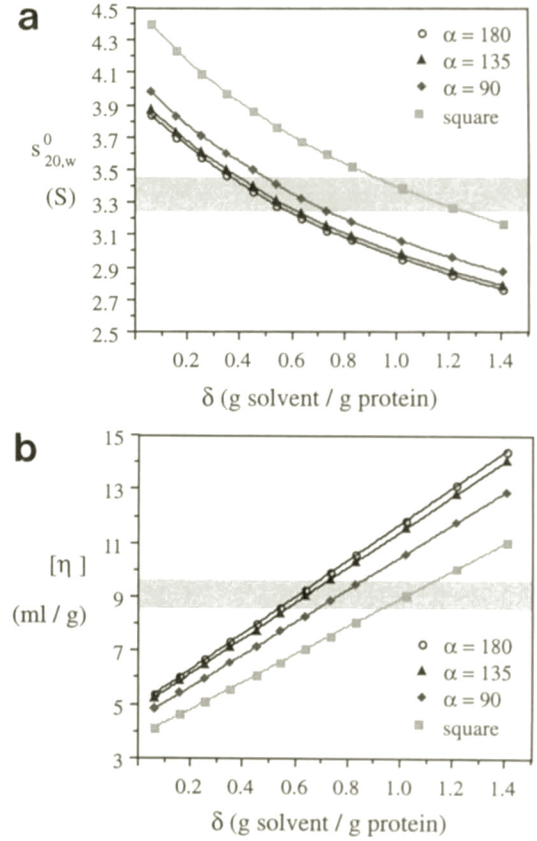

FIG. 6. *Panel a*, sedimentation coefficient ($s^0_{20,w}$) generated by hydrodynamic bead modeling, as a function of model hydration (δ) and intersegment angle (α). The *shaded area* represents the range of experimentally determined sedimentation coefficient ($s^0_{20,w}$ = 3.35 ± 0.1 S). *Panel b*, intrinsic viscosity [η] generated by hydrodynamic bead modeling as a function of hydration (δ) and intersegment angle (α). The *shaded area* represents the range of experimentally determined intrinsic viscosity ([η] = 9.1 ± 0.5 ml/g).

omer each with a randomly assigned intersegment angle. Instead we are asserting that a solution of monomer will contain molecules whose time-averaged conformation is characterized by the hydrodynamic parameters to which the bead model is constrained. Thus, requiring the model to conform to an $s^0_{20,w}$ = 3.35 ± 0.1 S (as previously measured for pneumolysin; Morgan *et al.* (1993)) and an intrinsic viscosity of [η] = 9.1 ± 0.5 ml/g, we observe from Fig. 6 (*a* and *b*) that the hydration must lie between 0.4 and 0.6 g of solvent/g of protein. It is evident that the sedimentation coefficient ($s^0_{20,w}$) is relatively insensitive to the intersegment angle (α). However, intrinsic viscosity ([η]) is a far more sensitive probe of conformation, as demonstrated by Fig. 6*b*, which illustrates the dependence of [η] upon α and hydration. We have also demonstrated that more compact conformations of the domains (exemplified by a square planar configuration for which predicted data are included in Fig. 6 (*a* and *b*)) are unlikely, as these would require an unreasonably high level of hydration. Recently the crystal structure of proaerolysin (Parker *et al.*, 1994), the toxin produced by the Gram-negative bacterium *Aeromonas hydrophila*, has been published. Proaerolysin has four domains, one of which is flexibly linked to the other three in a fashion that closely resembles our proposed structure for pneumolysin. Although proaerolysin has little sequence similarity to the thiol-activated toxins, the active form of the protoxin, aerolysin, does share a number of structural characteristics and biological functions. In particular it has a similar molecular weight (M_r = 48,000) and causes cytolysis. The oligomeric form of aerolysin is proposed to contain seven monomer subunits (Wilmsen *et al.*, 1992) arranged to form a 17-Å channel. This is significantly smaller than the oligomeric form of pneumolysin. On the basis of the low resolution images of the pneumolysin oligomer and the bead model of the monomer we propose the oligomeric model shown in Fig. 7 (*a* and *b*). The oligomer consists of about 30 subunits, arranged so that three of the domains lie adjacent to each other to form a cylindrical column and the fourth flexible domain forms a flange outside the cylinder. The resulting plan view appears as two concentric rings of subunits. This is consistent with the enhanced images presented for perfringolysin (Olofsson *et al.*, 1993) and streptolysin O (Sekiya *et al.*, 1993), which both indicate two concentric rings of subunits. However, the crucial difference is that we propose a single layer of subunits whose domain structure gives the appearance of a double ring. This model is similar to the models proposed for the C5b-9 complex (Tranum-Jensen *et al.*, 1978) and the aerolysin membrane channel (Wilmsen *et al.*, 1992).

We recognize that the precise orientation of the monomer subunits and their domains with respect to the membrane is

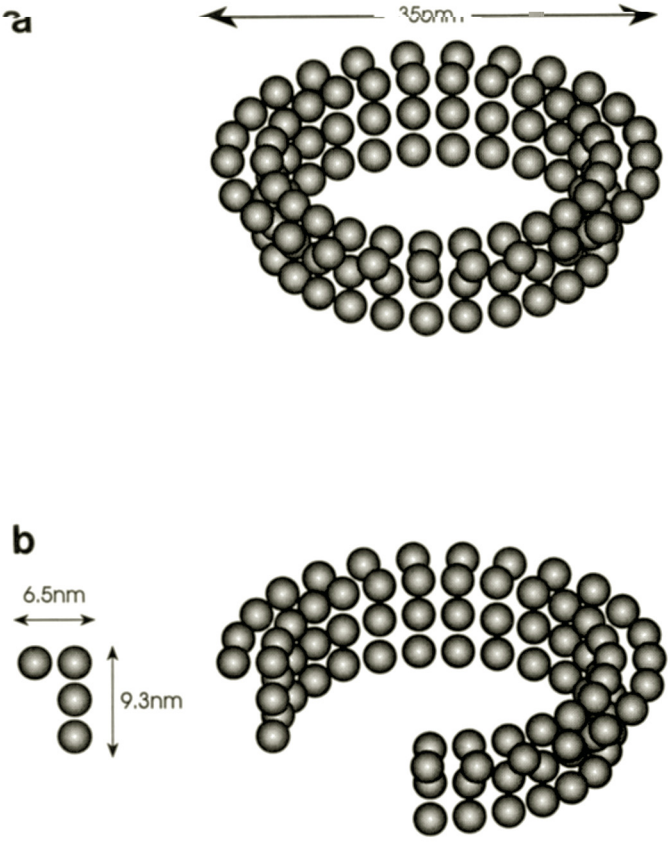

FIG. 7. **Bead model of pneumolysin oligomer.** *Panel a*, the dimensions of this model are based on measurements taken from the electron micrographs presented. Thus, based on the monomer bead model of Fig. 4*b*, we have fitted 26 monomers into the oligomeric model. A cut-away view is shown in *panel b* together with one of the removed monomers.

still unclear, and consequently a number of approaches are under way to refine these models. However, we suggest that these low resolution bead models provide a sensible platform on which to build more sophisticated models of these oligomers and further our knowledge of their assembly. We suggest that the proposed structures for pneumolysin will be relevant to other of the thiol-activated toxins.

REFERENCES

Alouf, J. E. & Geoffroy, C. (1991) in *Sourcebook of Bacterial Toxins* (Alouf, J. E. & Freer, J. H., eds) pp. 147–186, Academic Press, London

Austrian, R. (1981) *Rev. Infect. Dis.* **3,** 183–189

Berry, A. M., Yother, J., Briles, D. E., Hansman, D. & Paton, J. C. (1989) *Infect. Immun.* **57,** 2037–2042

Bhakdi, S., Tranum-Jensen, J. & Sziegoleit, A. (1985) *Infect. Immun.* **47,** 1, 52–60

Cowell, J. L., Kim, K. & Bernheimer, A. W. (1978) *Biochim. Biophys. Acta* **507,** 230–241

Dourmashkin, R. R. & Rosse, W. F. (1966) *Am. J. Med.* **41,** 699–710

Duncan, J. L. & Schlegel, R. (1975) *J. Cell Biol.* **67,** 160–173

García de la Torre, J. (1989) in *Dynamic Properties of Biomolecular Assemblies* (Harding, S. E. & Rowe, A. J., eds) pp. 3–31, Royal Society of Chemistry, Cambridge, United Kingdom

García de la Torre, J. & Bloomfield, V. A. (1981) *Q. Rev. Biophys.* **14,** 1, 671–674

Harris, R. W., Sims, P. J. & Tweten, R. K. (1991) *J. Biol. Chem.* **266,** 6936–6941

Klug, A. (1969) in *Nobel Symposium 11: Symmetry and Function of Biological Systems at the Macromolecular Level* (Engström, A. & Strandberg, B., eds) pp. 425–436, John Wiley and Sons, Inc., London, United Kingdom

Mitchell, T. J., Walker, J. A., Saunders, F. K., Andrew, P. W. & Boulnois, G. J. (1989) *Biochim. Biophys. Acta* **1007,** 67–72

Mitsui, K., Sekiya, T., Okamura, S., Nozawa, Y. & Hase, J. (1979) *Biochim. Biophys. Acta* **558,** 307–313

Morgan, P. J., Varley, P. G., Rowe, A. J., Andrew, P. W. & Mitchell, T. J. (1993) *Biochem. J.* **296,** 671–674

Morgan, P. J., Varley, P. G., Rowe, A. J., Hyman, S., Andrew, P. W. & Mitchell, T. J. (1994) in *Bacterial Protein Toxins: Supplement 24* (Freer, J., Aitkin, R., Alouf, J. E., Boulnois, G., Falmagne, P., Fehrenbach, F., Montecucco, C., Piemont, Y., Rappuoli, R., Wadström, T., and Witholt, B., eds) pp. 333–334, Gustav Fisher Verlag, Stuttgart

Niedermeyer, W. (1985) *Toxicon* **23,** 425–439

Olofsson, A., Hebert, H. & Thelestam, M. (1993) *FEBS Lett.* **319,** 125–127

Parker, M. W., Buckley, J. T., Postma, J. P. M., Tucker, A. D., Leonard, K., Pattus, F. & Tsernoglou, D. (1994) *Nature* **367,** 292–295

Rocco, M., Spotorno, B. & Hantgen, R. R. (1993) *Protein Sci.* **2,** 2154–2166

Rottem, S., Cole, R. M., Habig, W. H., Barile, M. F. & Hardegree, M. C. (1982) *J. Bacteriol.* **152,** 888–892

Rowe, A. J. (1984) in *Techniques in Protein and Enzyme Biochemistry* (Tipton, K. F., ed) Part I, suppl., pp. 29–32, Elsevier, Ireland

Saunders, F. K., Mitchell, T. J., Walker, J. A., Andrew, P. W. & Boulnois, G. J. (1989) *Infect. Immun.* **57,** 2547–2552

Sekiya, K., Satoh, R., Danbara, H. & Futaesaku, Y. (1993) *J. Bacteriol.* **175,** 5953–5961

Szuchet, S. & Johnson, P. (1966) *Eur. Polym. J.* **2,** 115–128

Tanford, C. (1955) *J. Phys. Chem.* **59,** 798

Tanford, C. (1963) *Physical Chemistry of Macromolecules*, John Wiley & Sons Inc., New York

Tranum-Jensen, J., Bhakdi, S., Bhakdi-Lehnen, B., Bjerrum, O. J. & Speth, V. (1978) *Scand. J. Immunol.* **7,** 45–56

Wilmsen, H. U., Leonard, K. R., Tichelaar, W., Buckley, J. T. & Pattus, F. (1992) *EMBO J.* **11, 7,** 2457–2463